Pertanika J. Sci. & Technol. 31 (3): 1325 - 1333 (2023)

SCIENCE & TECHNOLOGY

Journal homepage: http://www.pertanika.upm.edu.my/

Highly Conductive Graphenated-Carbon Nanotubes Sheet with Graphene Foliates for Counter Electrode Application in Dye-Sensitized Solar Cells

Yusnita Yusuf[1], Suhaidi Shafie[1,2]*, Ismayadi Ismail[1], Fauzan Ahmad[3], Mohd Nizar Hamidon[1,2], Pandey Shyam Sudhir[4] and Lei Wei[5]

[1]Institute of Nanoscience and Nanotechnology, Universiti Putra Malaysia, 43400 UPM, Serdang, Selangor, Malaysia
[2]Department of Electrical and Electronic Engineering, Faculty of Engineering, Universiti Putra Malaysia, 43400 UPM, Serdang, Selangor, Malaysia
[3]Malaysian-Japan International Institute of Technology, Universiti Teknologi Malaysia, 57000 UTM, Kuala Lumpur, Malaysia
[4]Graduate School of Life Science and System Engineering, Kyushu Institute of Technology, 2-4 Hibikino, Wakamatsu, Kitakyushu, Fukuoka 808-0196, Japan
[5]School of Electronic Science and Engineering, Southeast University, Sipailou, Jinling Yuan 109, Nanjing 210096, China

ABSTRACT

This work enlightened the synthesis of graphenated-carbon nanotubes sheet (g-CNT) using the floating-catalyst chemical vapor deposition method (FCCVD) for dye-sensitized solar cell (DSSC) application. The carbon injection flow rate in the experiment was varied to 6, 8, and 10 ml/h. The morphological findings revealed that the g-CNT formed a highly conductive network. Excellent conductivity was obtained for the sample g-CNT8 (34.5 S/cm) compared to the sample g-CNT6 (11.2S/cm) and CNT10 (4.76 S/cm). This excellent feature is due to the hybrid structure of the g-CNT8, which creates efficient electron transfer in the materials resulting in higher conductivity. The hybrid structure provides a high surface area that improves conductivity. Therefore, the g-CNT sheet is an excellent candidate to replace the conventional platinum used as a counter electrode (CE) in DSSC.

Keywords: Carbon-based counter electrode, DSSC, g-CNT sheet

ARTICLE INFO

Article history:
Received: 01 April 2022
Accepted: 07 September 2022
Published: 31 March 2023

DOI: https://doi.org/10.47836/pjst.31.3.12

E-mail addresess:
yusnita5890@gmail.com (Yusnita Yusuf)
suhaidi@upm.edu.my (Suhaidi Shafie)
ismayadi@upm.edu.my (Ismayadi Ismail)
mnh@upm.edu.my (Mohd Nizar Hamidon)
fauzan.kl@utm.my (Fauzan Ahmad)
shyam@life.kyutech.ac.jp (Pandey Shyam Sudhir)
lw@seu.edu.cn (Lei Wei)
*Corresponding author

ISSN: 0128-7680
e-ISSN: 2231-8526

INTRODUCTION

Brian O'Regan and Micheal Grätzel founded the dye-sensitized solar cells (DSSC) in 1991 (Andualem & Demiss, 2018) due to the advantages of DSSC, including easy fabrication, low-cost, light, and affordable sources of renewable energy (Muhammad et al., 2020; Lokman et al., 2021; Sharif et al., 2022). The main components of the DSSC structure are a photoanode, sensitizer, redox-mediator, and counter electrode (CE). The CE accumulates the electrons from the external circuit connected to the cell and reduces the redox pair reaction in the mediator. The oxidized redox pair is reduced by adding electrons from the CE surface. A large surface area at the interface region is required to provide more active reaction sites for this mechanism to work. Conventional platinum (Pt) CE is extensively used due to its outstanding conductivity and electrocatalytic ability (Hagfeldt et al., 2010). However, Pt-based CE is very expensive and highly resistant when corroded in an iodine electrolyte, which decomposes the Pt into PtI_4 (Olsen et al., 2000). These led many researchers to explore other low-cost materials with low resistance and excellent electrocatalytic ability. Nevertheless, many electrode materials with good catalytic properties do not have the competence for electron transfer.

Recently, extensive studies have investigated carbon-based CE materials, such as carbon nanotubes (CNT), carbon fibers, carbon black, graphene, and graphite (Yella et al., 2011) (Devadiga et al., 2021). Carbon materials are attractive as CE materials in DSSC due to their low-cost, impressive electrocatalytic activity, high corrosion resistance, and superior conductivity (Wu et al., 2017). Biswas et al. (2019) reported graphene/CNT-based CE and observed an efficiency of 4.66 % of that using Pt-based CE of 5.66 %. The hybrid carbon exhibits a promising potential to replace Pt-based CE in DSSC (Samantaray et al., 2020). Therefore, initiating the hybrid carbonaceous materials will effectively improve the charge transfer of conducting electrons (Chang et al., 2013; Yu et al., 2019).

Previously, our group has reported on the synthesis and characterization of a novel three-dimensional (3D) graphenated-carbon nanotube cotton (g-CNT) hybrid (Ismail et al., 2019). The g-CNT was synthesized without substrate using a single-step floating-catalyst chemical vapor deposition (FCCVD). The report showed a direct growth of hybrid g-CNT cotton and its injection flow rate on the g-CNT cotton development for applying gas sensors. The outcome revealed that the synthesized g-CNT hybrid could be applied as an electrode in electronic devices. Similar research on the g-CNT hybrid has been presented, including bilayer graphene/multiwalled-CNT(MWCNT) (Wahyuono et al., 2019) and graphene nanosheet/MWCNT (Ratul et al., 2019). However, studies on g-CNT sheet material for DSSC applications are scarce.

We predicted that the hybrid properties of the g-CNT sheet structure would provide a way to optimize the hybrid structure. It facilitates the charge transport for excellent conductivity than any of the two materials could achieve independently. Wan et al. (2013)

fabricated G/CNT nanowires via in situ joule heating and found an approximate resistance of 104 kΩ. (Wahyuono et al., 2019) demonstrated bilayer graphene/MWCNT and found that the electrode conductivity and the catalytic activity of graphene/MWCNT reduced the redox species within the electrolyte of the DSSC. Biswas et al. (2019) fabricated graphene nanosheet/MWCNT and found a sheet resistance of 123 Ω/sq, in which the graphene-MWCNT hybrid increased the conductivity. This work investigated the effect of g-CNT sheet morphology on its electrical conductivity. In the experiment, we synthesized the g-CNT sheet via a single-step process of the FCCVD method. The injection rate of the carbon source is expected to be a parameter in the synthesis that influences the materials' morphology. For comparison, a standard CNT sheet was used to prove our hypothesis.

MATERIALS AND METHODS

Synthesis of the g-CNT Sheet by FCCVD

This experiment synthesized g-CNT and CNT sheets via the FCCVD method. A similar synthesis of our CNT was also reported in the literature (Yusuf et al., 2021; Ismail et al., 2019; Ibrahim et al., 2019; Ismail et al., 2018; Adnan et al., 2015). We introduced mix gases of argon, Ar (200 sccm) and hydrogen, H_2 (100 sccm) as the carrier gas, thiophene as the promoter, ferrocene as the catalyst (2.4 wt %), and ethanol as the carbon feedstock. Firstly, the promoter was mixed in ethanol and sonicated for dispersion. The synthesis was started with argon flow at 200 sccm to eliminate the oxygen from the furnace reactor at 600°C until it reached 1150°C and then changed to H_2 gas flow at 100 sccm. The synthesis was then carried out using an electronic syringe pump to inject the carbon feedstock for 2 hours. Other synthesis parameters were fixed, such as temperature, catalyst, and gas flow rate. The carbon injection flow rate was varied; 6 and 8, and 10 ml/h. H_2 gas was stopped during the cooling process, and argon gas flow was used. The samples were produced in cotton bulk form during the synthesis. After the synthesis, it was compressed into a sheet form, as shown in Figure 1. The g-CNT and CNT sheets were then cut into the dimension of 1 cm^2 for characterization. The samples were nominated as follows; g-CNT 6 ml/hr as g-CNT6, g-CNT 8 ml/hr as g-CNT8, and CNT 10ml/hr as CNT10.

Material Characterizations

The morphology of the samples was studied by FESEM (FEI NovaNanoSem 230) and HRTEM (Jeol JEM-2100F). The graphitized samples were characterized by Raman spectroscopy (WITec model Alpha 300R) at 532 nm excitation wavelength. The electrical conductivity was measured using a four-point probe (Loresta-GX MCP-T700, Mitsubishi Chemical Analytech). The thermal stability was measured by thermogravimetric analysis (TGA) (Mettler Toledo) at a heating rate of 20°C/min and temperature of 1000°C under oxygen conditions.

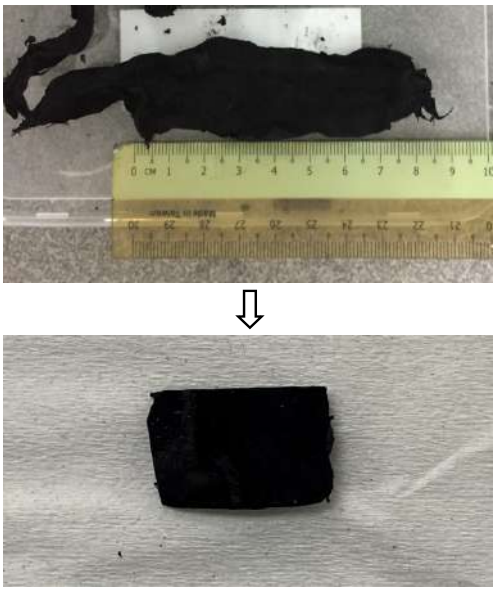

Figure 1. Synthesized g-CNT cotton was pressed into the g-CNT cotton sheet

RESULTS AND DISCUSSION

Morphological Study of g-CNT Sheet Analysis

The FESEM images of g-CNT6 and g-CNT8 in Figures 2a and 2b display a similar structure. They formed a long, thread-like structure and twisted with one another to form the cotton structure of the samples. The respective average diameter (obtained from Image J software) of 0.04 µm and 0.65 µm for samples g-CNT6 and g-CNT8 consists of g-CNT foliates growing from the sidewalls of multi-wall CNTs. Figure 2a shows the density of foliates with some clusters of nanotubes, while Figure 2b shows packed foliates and nanotubes clusters. The structure difference is attributed to the different injection rates during synthesis. The morphology of CNT10 obtained an average diameter of 0.34 µm and non-uniform nanotube growth owing to inadequate sulfur during the reaction (Ismail et al., 2019).

The morphology was observed to form an excellent conductive network of g-CNT. The networks provide a shorter route for electron transfer to increase conductivity. The fundamental advantage of the hybrid g-CNT structure is the high surface area of the three-dimensional framework of the CNTs (Parker et al., 2012). The high edge density of graphene can significantly increase the total charge capacity per unit of nominal area compared to other carbon nanostructures (Parker et al., 2012). The HRTEM image in Figures 2d and 2e showed the graphene foliates with both edges and basal planes of the CNT having an average foliate size of 137.88 nm.

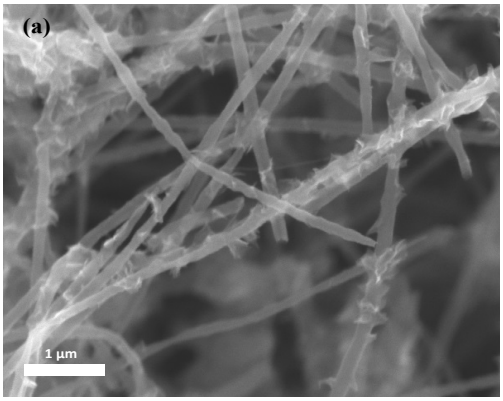

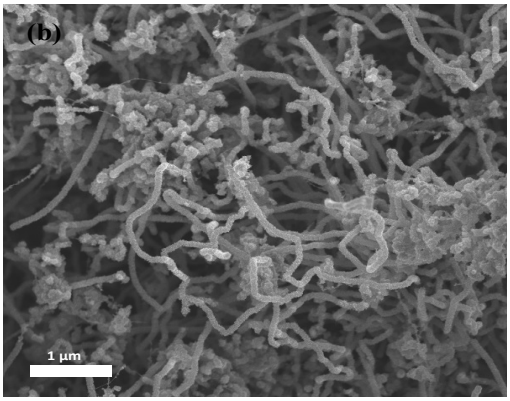

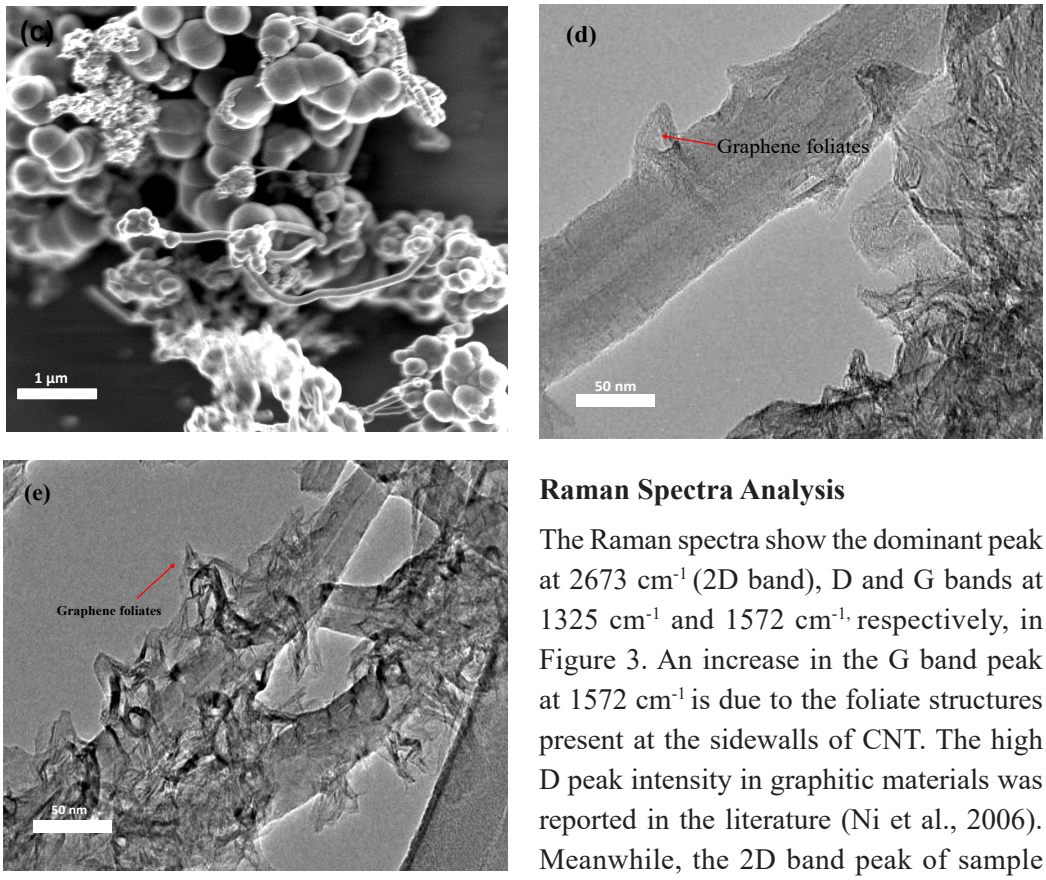

Figure 2. FESEM images of (a) g-CNT6, (b) g-CNT8, (c) CNT10, and HRTEM images of (d) g-CNT6, (e) g-CNT8.

Raman Spectra Analysis

The Raman spectra show the dominant peak at 2673 cm^{-1} (2D band), D and G bands at 1325 cm^{-1} and 1572 $cm^{-1,}$ respectively, in Figure 3. An increase in the G band peak at 1572 cm^{-1} is due to the foliate structures present at the sidewalls of CNT. The high D peak intensity in graphitic materials was reported in the literature (Ni et al., 2006). Meanwhile, the 2D band peak of sample g-CNT8 was increased due to single-layer graphene.

The I_D/I_G ratio for synthesized nanomaterial was 1.06 (g-CNT8, 0.98 (g-CNT6), and 0.99 (CNT10) (Ismail et al., 2019; Abdullah et al., 2021). The intensities of I_D/I_G indicated the lower quality of sp^2 carbon structures when the ratio of I_D/I_G is high (Wepasnick et al., 2010). The higher ratio of defects can improve the exchange current density and electrical conductivity at the interface to improve the catalytic activity of redox reaction according to the catalytic function of CE in DSSC (Chang et al., 2013; Yu et al., 2019). The high ratio is attributed to the growth of graphene foliates at the CNT sidewalls, as agreed in Figure 2. It was also due to graphene structures being higher than the defect. These would help electron mobility move easily through the graphitic interfacial layer because of lower barrier resistance (Ismail et al., 2019).

The absence of radial breathing modes (RBM) peaks at lower wavenumber, suggesting that the samples are multi-walled CNT (Adnan et al., 2015; Ibrahim et al., 2019). It is agreed from the microstructural analysis.

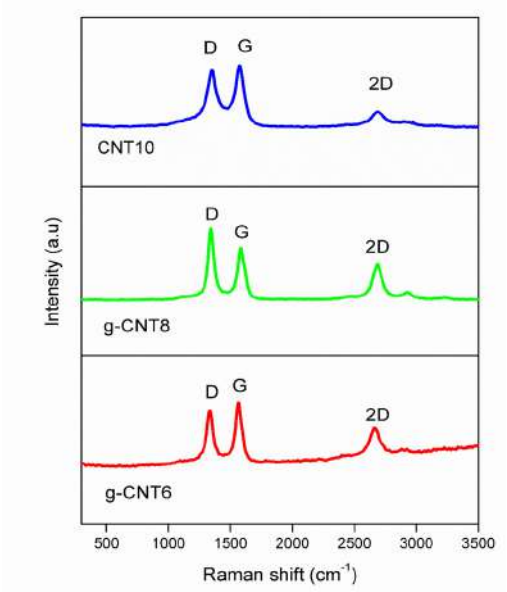

Figure 3. Raman spectra of g-CNT6, g-CNT8, and CNT10.

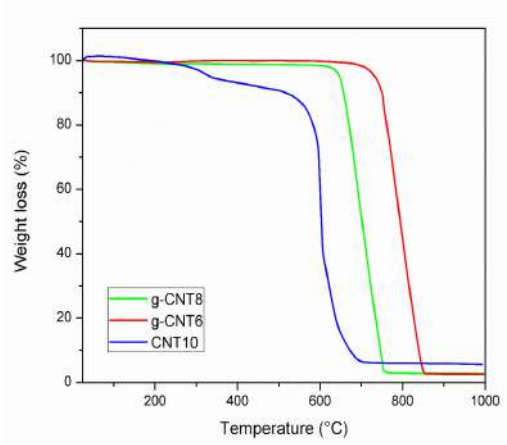

Figure 4. TGA results for g-CNT6, g-CNT8, and CNT10.

Thermogravimetric Analysis

The TGA shown in Figure 4 provides the details of the decomposition temperature of the samples. The TGA analysis can help find the optimal firing temperature for the preparation of the counter electrode. The initial weight begins to lose approximately 400°C because of the elimination of absorbed water and the oxidation of volatile carbon content (Adnan et al., 2015). The rapid weight loss between the temperature of 620 to 860°C was caused by the oxidation of the amorphous carbon. The decomposition seem comparable with result obtained from the previous work (Ismail et al., 2019). In the sample g-CNT6, the thermal stability was observed from 30°C up to 700°C, and after 710°C, weight loss started to decrease significantly. The thermal stability for sample g-CNT8 begins from 30°C up to 610°C, and beyond this temperature, it begins to lose weight. However, for CNT10, the thermal stability decreased at 500°C. These decomposition was similar as reported by (Ibrahim et al., 2019) which indicated that CNT10 are stable up to ~500 °C. We observed that the CNT sheets possess high thermal stability, with g-CNT6 being the most thermally stable. The remaining weight after being sintered at 1000°C was approximately 2.54 wt%, while the g-CNT8 displays 2.71 wt% and CNT10 5.58 wt%.

Electrical Conductivity Analysis

The electrical properties shown in Table 1 provide information regarding the samples' electrical conductivity, resistivity, and sheet resistance. The measurement was conducted using rectangular probes, and the samples were cut into a dimension of 1 cm^2. The results showed that g-CNT8 possessed higher electrical conductivity (34.5 S/cm) than g-CNT6

Table 1
Electrical conductivity analysis

	Sheet resistance (Ω/sq)	Resistivity (Ω.cm)	Conductivity (S/cm)
g-CNT6	3.00	8.93×10^{-2}	11.2
g-CNT8	0.90	2.90×10^{-2}	34.5
CNT10	6.78	0.21	4.76

(11.2 S/cm) and CNT10 (4.76 S/cm). The lower sheet resistance obtained from sample g-CNT8 (0.9 Ω/sq) compared with g-CNT6 (3.0 Ω/sq) and CNT10 (6.78 Ω/sq) resulted in higher conductivity. The existing literature reported that the increase in diameter would decrease the resistivity (Collins et al., 1997). These agree with our FESEM images from Figure 2, in which g-CNT6 and g-CNT8 samples have increased diameters of the g-CNT sheets.

Furthermore, due to the growth of graphene foliates at the sidewalls of CNT, the chemical bond of these materials creates a more charge transfer resulting in higher conductivity (Parker et al., 2012). In DSSC applications, such excellent electrical conductivity performance can promote faster redox reactions and efficiently regenerate the electrons to supply back into the cell. From this measurement, the sample g-CNT8 can be a potential material to substitute platinum as the conventional CE for DSSC.

CONCLUSION

In conclusion, g-CNT and CNT sheets were successfully synthesized via the FCCVD method. The morphology structure of the g-CNT sheet revealed foliates growing out from the sidewalls of multi-walled CNT. The g-CNT6 showed more stability than the g-CNT8 and CNT10. High conductivity was obtained for the sample g-CNT8 (34.5 S/cm) compared to the sample g-CNT6 (11.2 S/cm) and CNT10 (4.76 S/cm). The hybrid structure of the g-CNT sheet creates efficient charge transfer in the materials resulting in higher conductivity. Thus, the g-CNT sheet, especially g-CNT8, can potentially substitute platinum as the conventional CE in DSSC.

ACKNOWLEDGMENT

The authors thank the Institute of Nanoscience and Nanotechnology (ION2), Universiti Putra Malaysia (UPM), for providing the experimental facilities and services. This study was funded by the UniPutra Berimpak grant (Vot: 9689000) and Universiti Putra Malaysia (UPM), and Kyushu Institute of Technology Japan (Kyutech) through (UPM-Kyutech/2019/9300465) grant.

REFERENCES

Abdullah, H. B., Irmawati, R., Ismail, I., Zaidi, M. A., & Abdullah, A. A. A. (2021). Synthesis and morphological study of graphenated carbon nanotube aerogel from grapeseed oil. *Journal of Nanoparticle Research*, *23*(11), Article 244. https://doi.org/10.1007/s11051-021-05363-6

Adnan, N. L., Ismail, I., & Hashim, M. (2015). Effect of ferrocene concentration on the carbon nanotube cotton synthesized via floating catalyst CVD method. *Australian Journal of Basic and Applied Sciences*, *9*(12), 109-113.

Andualem, A., & Demiss, S. (2018). Review on dye-sensitized solar cells (DSSCs). *Edelweiss Applied Science and Technology*, *2*(1), 145-150. https://doi.org/10.33805/2639-6734.103

Biswas, R. K., Nemala, S. S., & Mallick, S. (2019). Platinum and transparent conducting oxide free graphene-CNT composite based counter-electrodes for dye-sensitized solar cells. *Surface Engineering and Applied Electrochemistry*, *55*(4), 472-480. https://doi.org/10.3103/S1068375519040021

Chang, L. H., Hsieh, C. K., Hsiao, M. C., Chiang, J. C., Liu, P. I., & Ho, K. K. (2013). A graphene-multi-walled carbon nanotube hybrid supported on fluorinated tin oxide as a counter electrode of dye-sensitized solar cells. *Journal of Power Sources*, *222*, 518-525. https://doi.org/10.1016/j.jpowsour.2012.08.058

Collins, P. G., Zettl, A., Bando, H., Thess, A., & Smalley, R. E. (1997). Nanotube nanodevice. *Science*, *278*(5335), 100-103. https://doi.org/10.1126/science.278.5335.100

Devadiga, D., Selvakumar, M., Shetty, P., & Santosh, M. S. (2021). Dye-sensitized solar cell for indoor applications: A mini-review. *Journal of Electronic Materials*, *50*(6), 3187-3206. https://doi.org/10.1007/s11664-021-08854-3

Hagfeldt, A., Boschloo, G., Sun, L., Kloo, L., & Pettersson, H. (2010). Dye-sensitized solar cells. *Chemical Reviews*, *110*(11), 6595-6663. https://doi.org/10.1021/cr900356p

Ibrahim, N. I., Ismail, I., Mamat, S. M., & Adnan, N. L. (2019). Effect of carbon source injection rate on CNT film via floating catalyst CVD method. *Solid State Phenomena*, *290*, 113-121. https://doi.org/10.4028/www.scientific.net/ssp.290.113

Ismail, I., Yusof, J. M., Nong, M. A. M., & Adnan, N. L. (2018). Synthesis of carbon nanotube-cotton superfiber materials. In *Synthesis, Technology and Applications of Carbon Nanomaterials* (pp. 61-76). Elsevier. https://doi.org/10.1016/b978-0-12-815757-2.00003-6

Ismail, I., Mamat, S., Adnan, N. L., Yunusa, Z., & Hasan, I. H. (2019). Novel 3-dimensional cotton-like graphenated-carbon nanotubes synthesized via floating catalyst chemical vapour deposition method for potential gas-sensing applications. *Journals of Nanomaterials*, *2019*, 1-10. https://doi.org/10.1155/2019/5717180

Lokman, M. Q., Shaban, S., Shafie, S., Ahmad, F., Yahaya, H., Mohd Rosnan, R., & Ibrahim, M. A. (2021). Improving Ag-TiO_2 nanocomposites' current density by $TiCl_4$ pretreated on FTO glass for dye-sensitised solar cells. *Micro & Nano Letters, 16*(7), 381-386. https://doi.org/10.1049/mna2.12061

Muhammad, N. Y., Mohtar, M. N., Ramli, M. M., Shafie, S., Shaban, S., & Yusuf, Y. (2020). *Enhancement of dye sensitized solar cell by adsorption of graphene quantum dots*. *International Journal of Materials, Mechanics and Manufacturing, 8*(3), 126-130. https://doi.org/10.18178/ijmmm.2020.8.3.494

Ni, Z. H., Fan, H. M., Feng, Y. P., Shen, Z. X., Yang, B. J., & Wu, Y. H. (2006). Raman spectroscopic investigation of carbon nanowalls. *The Journal of Chemical Physics, 124*(20), Article 204703. https://doi:10.1063/1.2200353

Olsen, E., Hagen, G., & Lindquist, S. E. (2000). Dissolution of platinum in methoxy propionitrile containing LiI/I_2. *Solar Energy Materials and Solar Cells*, *63*(3), 267-273. https://doi.org/10.1016/S0927-0248(00)00033-7

Parker, C. B., Raut, A. S., Brown, B., Stoner, B. R., & Glass, J. T. (2012). Three-dimensional arrays of graphenated carbon nanotubes. *Journal of Materials Research*, *27*(7), 1046-1053. https://doi.org/10.1557/jmr.2012.43

Samantaray, M. R., Mondal, A. K., Murugadoss, G., Pitchaimuthu, S., Das, S., Bahru, R., & Mohamed, M. A. (2020). Synergetic effects of hybrid carbon nanostructured counter electrodes for dye-sensitized solar cells : A review. *Materials*, *13*(12), Article 2779. https://doi.org/10.3390/ma13122779

Sharif, N. F. M., Kadir, M. Z. A. A., Shafie, S., Din, M. F., Yusuf, Y., & Samaila, B. (2022). Light absorption enhancement using graphene quantum dots and the effect of N-719 dye loading on the photoelectrode of dye-sensitized solar cell (DSSC). *Key Engineering Materials*, *908*, 259-264. https://doi.org/10.4028/p-0cm1r4

Wahyuono, R. A., Jia, G., Plentz, J., Dellith, A., Dellith, J., Herrmann-Westendorf, F., Dietzek, B. (2019). Self-assembled graphene/MWCNT bilayers as platinum-free counter electrode in dye-sensitized solar cells. *ChemPhysChem*, *20*(24), 3336-3345. https://doi.org/10.1002/cphc.201900714

Wan, N., Sun, L. T., Ding, S. N., Xu, T., Hu, X. H., Sun, J., & Bi, H. C. (2013). Synthesis of graphene-CNT hybrids via joule heating: Structural characterization and electrical transport. *Carbon*, *53*, 260-268. https://doi.org/10.1016/j.carbon.2012.10.057

Wepasnick, K. A., Smith, B. A., Bitter, J. L., & Fairbrother, D. H. (2010). Chemical and structural characterization of carbon nanotube surfaces. *Analytical and Bioanalytical Chemistry*, *396*(3), 1003-1014. https://doi.org/10.1007/s00216-009-3332-5

Wu, J., Lan, Z., Lin, J., Huang, M., Huang, Y., Fan, L., Wei, Y. (2017). Counter electrodes in dye-sensitized solar cells. *Chemical Society Reviews*, *46*(19), 5975-6023. https://doi.org/10.1039/c6cs00752j

Yella, A., Lee, H. W., Tsao, H. N., Yi, C., Chandiran, A. K., Nazeeruddin, M. K., Grätzel, M. (2011). Porphyrin-sensitized solar cells with cobalt (II/III)–based redox electrolyte exceed 12 percent efficiency. *Science*, *334*, 629-633. https://doi.org/10.1126/science.1209688

Yu, F., Shi, Y., Yao, W., Han, S., & Ma, J. (2019). A new breakthrough for graphene/carbon nanotubes as counter electrodes of dye-sensitized solar cells with up to a 10.69% power conversion efficiency. *Journal of Power Sources*, *412*, 366-373. https://doi.org/10.1016/j.jpowsour.2018.11.066

Yusuf, Y., Shafie, S., Ismail, I., Ahmad, F., Hamidon, M. N., Pandey, S. S., Lei, W. (2021). A comparative study of graphenated-carbon nanotubes cotton and carbon nanotubes as catalyst for counter electrode in dye-sensitized solar cells. *Malaysian Journal of Microscopy*, *17*(2), 162-174. https://malaysianjournalofmicroscopy.org/ojs/index.php/mjm/article/view/543